Open access • Journal Article • DOI:10.1002/PSSA.201127060

Structure and optical properties of silicon layers with GaSb nanocrystals created by ion-beam synthesis — Source link

F. F. Komarov, L. Vlasukova, O. Milchanin, A. V. Mudryi ...+3 more authors

Institutions: Belarusian State University, National Academy of Sciences of Belarus, University of Jena

Published on: 01 Jan 2012 - Physica Status Solidi (a) (WILEY-VCH Verlag)

Topics: Photoluminescence and Silicon

Related papers:

- Formation of InAs nanocrystals in Si by high-fluence ion implantation
- The Comparative Investigations of Structural and Optical Properties of GaSb Nanocrystals/Si Layers
- Photoluminescence and Raman scattering of silicon nanocrystals prepared by silicon ion implantion into SiO2 films
- Structural and optical properties of silicon layers with InSb and InAs nanocrystals formed by ion-beam synthesis
- Optical and Structural Properties of Silicon with Ion-Beam Synthesized InSb Nanocrystals

Share this paper:

View more about this paper here: https://typeset.io/papers/structure-and-optical-properties-of-silicon-layers-with-gasb-59q5hdijiw

reprint

WILEY-VCH

Phys. Status Solidi A **209**, No. 1, 148–152 (2012) / **DOI** 10.1002/pssa.201127060

Structure and optical properties of silicon layers with GaSb nanocrystals created by ion-beam synthesis

F. Komarov*[,1], L. Vlasukova[1], O. Milchanin[1], A. Mudryi[2], B. Dunets[1], W. Wesch[3], and E. Wendler[3]

[1] Belarusian State University, Nezavisimosti Ave. 4, 220030 Minsk, Belarus
[2] Scientific and Practical Materials Research Centre, National Academy of Sciences of Belarus, P. Brovki Str. 17, 220072 Minsk, Belarus
[3] Institut für Festkörperphysik, Friedrich-Schiller-Universität Jena, Max-Wien-Platz 1, 07743 Jena, Germany

Received 8 February 2011, revised 9 June 2011, accepted 21 September 2011
Published online 17 October 2011

Keywords crystalline silicon, GaSb nanocrystals, high-fluence implantation, thermal treatment

* Corresponding author: e-mail komarovf@bsu.by, Phone: +375(172)12 48 33, Fax: +375(172)78 04 17

We have studied the ion-beam synthesis of GaSb nanocrystals in Si by high-fluence implantation of Sb and Ga ions followed by thermal annealing. RBS, TEM/TED, RS, and photoluminescence (PL) were employed to characterize the implanted layers. It was found that the nanocrystals size increases from 5 to 60 nm in the samples annealed at 900 °C up to 20–90 nm in the samples annealed at 1100 °C. An existence of significant mechanical stresses within implanted layers has been detected. The stress values have been calculated from the shift of the Si first order Raman band. For the samples annealed at 900 °C a broad band in the spectral region of about 0.75–1.05 eV is detected in the PL spectra. The nature of this PL band is discussed.

© 2011 WILEY-VCH Verlag GmbH & Co. KGaA, Weinheim

1 Introduction GaSb is a direct band-gap A^3B^5 semiconductor with a narrow band-gap of about 0.75 eV. The synthesis of GaSb quantum dots inside the crystalline Si is of interest for applications in light emitting diodes and photodetectors operating in the IR range. InAs clusters have been formed on Si (001) by MBE-technique [1]. Such clusters covered with a Si cap layer show intense luminescence at 1.3 μm at 7 K. Light emitting diodes containing GaSb-quantum dots embedded in Si and operating at room temperature have been reported also [2]. Samples with GaSb-quantum dots were grown by MBE-technique on p-type Si (001). Post-growth annealing of these structures resulted in an appearance of a sharp line of luminescence localized at 900-meV [2]. The other technique for fabricating III–V quantum dots is ion-beam synthesis of nanocrystals by means of ion implantation followed by thermal treatment. In this technique, high-fluence ion implantation produces a supersaturation of one or more implanted species in the near-surface of crystalline or amorphous matrix. The embedded impurities then form precipitates within the host during thermal processing at elevated temperatures. InAs nanoclusters have been formed using this method in SiO_2 and Si [3–5]. Unfortunately, thermal processing of implanted crystals results not only in precipitation and radiation damage recovery. Negative consequences of thermal processing exist such as a broadening of depth concentration profiles of embedded impurity and a net loss of implanted atoms because of diffusion that is favored at elevated temperature. Radiation defects are also taking part in the diffusion redistribution of embedded foreign atoms. Thus, on the one hand complex defect structures are formed during implantation and annealing at elevated temperatures, which significantly influence the formation, the size, and the depth distribution of the precipitates. On the other hand, the existence of the precipitates has also a strong effect on the quality of the surrounding crystalline host after the post-implantation annealing.

The purpose of this paper is to investigate the effect of post-implantation thermal processing on the diffusion redistribution of embedded foreign atoms and on the structural and optical properties of Si implanted with high fluence of both Sb and Ga ions.

2 Experimental The samples with the size of about $1 \times 1\ cm^2$ were cut out of n-Si(001) wafer and subsequently implanted with Sb (250 keV, $5 \times 10^{16}\ cm^{-2}$) and Ga ions

© 2011 WILEY-VCH Verlag GmbH & Co. KGaA, Weinheim

(350 keV, $5 \times 10^{16}\,\mathrm{cm}^{-2}$) at 500 °C. The samples were implanted under an angle of 7° with respect to the surface normal without rotation. Afterwards, the samples were annealed using conventional furnace annealing and rapid thermal annealing (RTA) in inert ambient.

In order to analyze a depth distribution of the implanted atoms as well as to evaluate the damage of the implanted material, we applied Rutherford backscattering spectrometry in the combination with the channeling technique (RBS/C). RBS measurements were performed with 1.3 MeV He^+. The calculation of Sb and Ga concentrations in Si by RBS spectra is complicated by the overlapping of Ga and Sb peaks. To solve this problem, we measured RBS spectra at two angles of the incidence of He^+ ions into the samples: 0 and 50° (in Kernel geometry).

The depth profiles of the implanted ions were obtained by simulation of spectra until they coincided completely with the experimental spectra recorded at two angles (0 and 50°).

Structural modifications after implantation and annealing were studied by means of transmission electron microscopy (TEM) and diffraction (TED). The TEM investigations in plan view (PV) geometry were performed using a 200 keV-Hitachi H-800. In order to obtain information from different depths the PV-TEM sample preparation was combined with a precise etching technique which allows stepwise clearing away defined thin layers.

The optical properties of samples were investigated by Raman spectroscopy (RS) and photoluminescence (PL).

Micro-Raman scattering experiments were carried out using a RAMANOR U-1000 dispersive spectrometer. The samples were excited with a laser beam ($\lambda = 532$ nm) and the scattered light was detected in backscattering geometry. Raman spectra were recorded within the wave number range from 90 to 600 cm^{-1} at room temperature. PL spectra were recorded in the spectral region of 0.7–2 eV using a 0.6 m grating monochromator and a cooled InGaAs detector. During the measurements the samples were mounted in a liquid He immersion cryostat, the 514.5 nm line of an argon ion laser was used to excite PL.

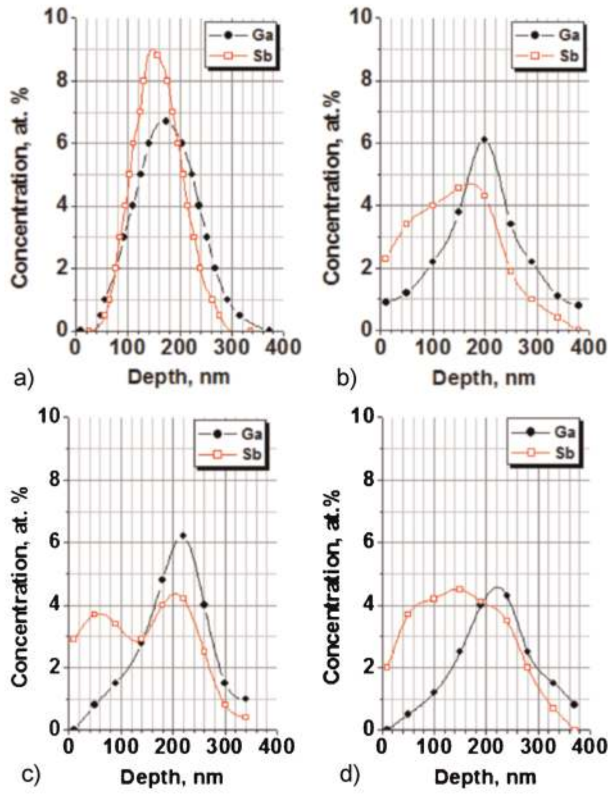

Figure 1 (online color at: www.pss-a.com) Distribution of impurities along the sample depth of Si implanted with Sb (350 keV, $5 \times 10^{16}\,\mathrm{cm}^{-2}$) and Ga ions (250 keV, $5 \times 10^{16}\,\mathrm{cm}^{-2}$) at 500 °C: (a) calculated with SRIM 2003, (b–d) calculated from the RBS spectra depth profiles with (b) giving the result for as-implanted sample, (c) after furnace annealing (900 °C, 45 min), and (d) giving the result for the sample after RTA (900 °C, 30 s).

3 Results and discussion

Figure 1 shows the depth profiles of Ga and Sb atoms in as-implanted and annealed samples, which were calculated from the RBS spectra. For comparison Fig. 1a depicts the ion distributions calculated with the computer code SRIM'2003. From Fig. 1b one can see that implantation at 500 °C already leads to strong broadening and significant reduction of the impurity concentration as compared to the SRIM calculation. This effect is weaker for Ga than for Sb. The Sb depth profile shows an asymmetric broadening toward the surface of the sample.

The melting temperature of GaSb is 712 °C. In order to achieve a recovery of Si structure as complete as possible without GaSb melting, a first set of samples was annealed at 700 °C for 45 min. PL spectra of the implanted samples are presented in Fig. 2. One can see that a broad asymmetric band with a maximum at 0.91 eV dominates in the PL spectrum of the as-implanted sample (Fig. 2a). Annealing at 700 °C leads to the disappearance of this band and to the appearance of an intensive band of exciton emission in Si peaked at 1.09 eV and less intensive bands at 1.03 and 1.14 eV. We did not succeed to get channeled RBS spectra from the samples annealed at 700 °C, what indicates an insufficient structural recovery of the implanted layers. Therefore, the implanted crystals were annealed at a temperature of 900 °C which exceeds the melting point of GaSb. The resulting depth profiles of the implanted species are presented in Fig. 1c and d. One can see that RTA leads to a strong broadening of the Sb profile toward the surface in comparison to the as-implanted sample. An increase of the thermal processing duration to 45 min results in a bimodal distribution of Sb atoms with maxima at 50 and 200 nm. A mechanism of such Sb redistribution after an annealing is not clear. We suppose that an evolution of defect structure during an annealing causes such abnormal Sb diffusion to the surface. A similar bimodal distribution of species in Si implanted at 550 °C with high fluence of Zn^+ or Ag^+ ions and annealed at 700 °C for 20 h was earlier reported by Meldrum et al. [6]. Authors of Ref. [6] extracted depth concentration profiles of

© 2011 WILEY-VCH Verlag GmbH & Co. KGaA, Weinheim

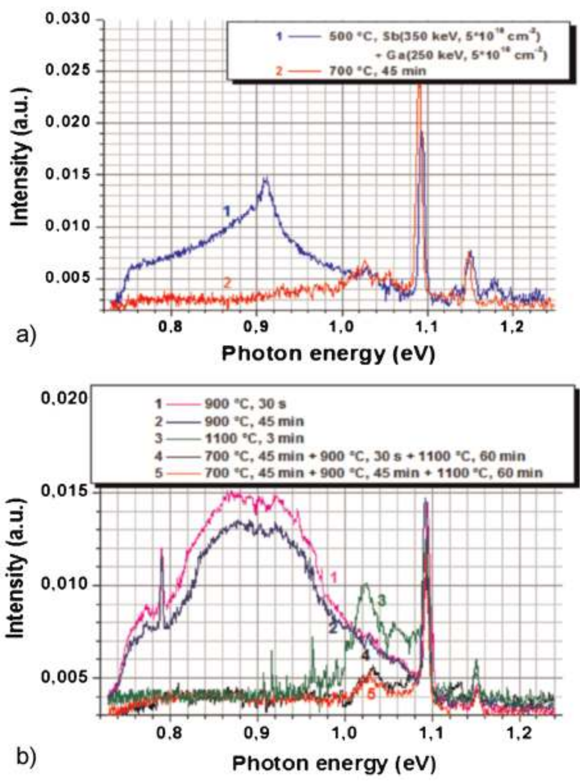

Figure 2 (online color at: www.pss-a.com) PL spectra of Si samples implanted with Sb and Ga and annealed in different regimes.

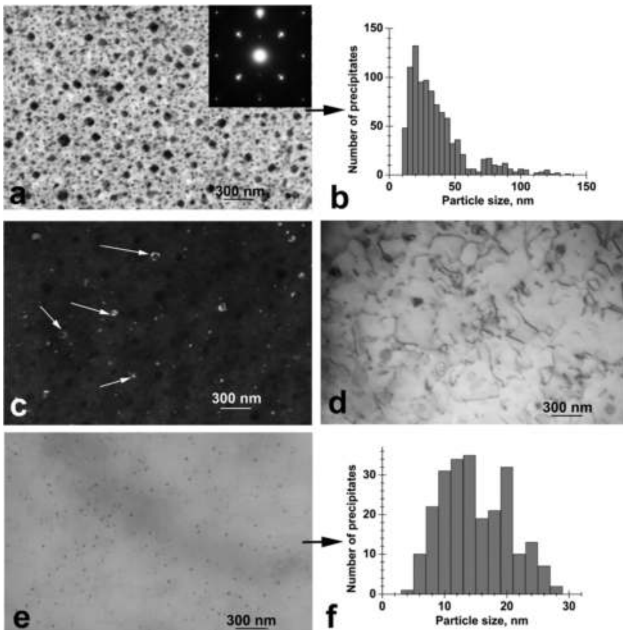

Figure 3 Bright-field (a, d, and e) and dark-field (c) TEM-images from Si after "hot" implantation of Sb (350 keV, $5 \times 10^{16}\,cm^{-2}$) and Ga (250 keV, $5 \times 10^{16}\,cm^{-2}$) and heat treatment (900 °C, 45 min) and precipitate size distributions (b and f). The sample after the removal of surface layer of 190 nm thickness (d–f).

impurities from RBS spectra, too, and attributed such "two-peak" structure of these distributions to diffusion of impurity away from the peak of the implant concentration and toward the peak damage region at a shallower depth.

Figures 3 and 4 shows TEM-images and precipitate size distributions of Si implanted with Sb and Ga and annealed in different modes. We have not observed an amorphization of subsurface Si layer after "hot" implantation of Sb and Ga ions. Though, an implanted layer is characterized by essential damage. The annealing leads to substantial structure recovery. The surface region of the samples annealed at 900 °C for 45 min is a damaged layer containing microtwins and precipitates (Fig. 3a and c). The existence of a great number of microtwins may be caused by subsurface Sb atoms accumulation that is registered by RBS (Fig. 1b). It should be noted a bimodal size distribution of precipitates (a diffraction contrast from that ones did not disappear during sample tilting – Fig. 3a and b) for the sample annealed at 900 °C for 45 min. The most of precipitates have a size between 10 and 50 nm. Though, a part of ones has a size from 70 to 100 nm. One can see small extra reflexes beside basic Si matrix reflexes at electron diffraction pattern (inset in Fig. 3a). These extra reflexes location is similar to the location of twin Si reflexes. Figure 3c shows a dark-field image taken in ⟨220⟩-reflex of Si along with such extra-reflex. One can see an interesting effect – "lighting" of nanocluster/Si interfaces (marked by arrows in Fig. 3c).

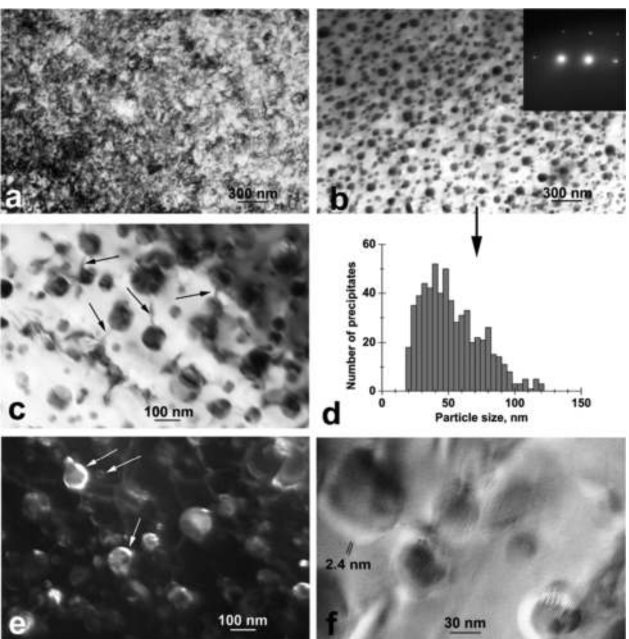

Figure 4 Bright-field (a–c and f) and dark-field (e) TEM-images from Si after "hot" implantation of Sb (350 keV, $5 \times 10^{16}\,cm^{-2}$) and Ga (250 keV, $5 \times 10^{16}\,cm^{-2}$) and heat treatment at 900 °C, 30 s (a) and 1100 °C, 60 min (b, c, e, and f), and precipitate size distribution (d). The sample after the removal of 190 nm layer (a) and the sample without the removal of surface layer (b–f).

© 2011 WILEY-VCH Verlag GmbH & Co. KGaA, Weinheim

According to the RBS data a maximum of embedded atoms is located at the depth of about 200 nm. In order to investigate the structure of the implanted layer at this depth in detail, we have removed nearly 190 nm from the surface of selected samples by chemical etching. In the sample which was annealed at 900 °C for 45 min, small precipitates and dislocation-like defects (dislocations and dislocation loops) can be distinguished after the 190 nm-layer removing (Fig. 3d). In order to investigate precipitates in detail we have varied a samples tilt and got images without a diffraction contrast from dislocations. Figure 3e shows TEM-image of thinned sample taken at such conditions. In accordance with the size distribution (Fig. 3f), the range of precipitates sizes are remarkably reduced in deeper regions of the sample, with the size being equal to 5–30 nm.

Figure 4a depicts TEM-image of the sample annealed at 900 °C for 30 s applying RTA after the 190 nm layer removing. One can see that it is very difficult to distinguish precipitates and microtwins in this case. Hence, the total damage level in the sample after RTA is substantially higher in comparison with the sample subjected to the longer furnace annealing at the same temperature (900 °C). Though, PL spectra of the both samples are the same and characterized with a narrow band of exciton emission in Si at 1.09 eV and a broad band at 0.75–1.05 eV (Fig. 2b). A similar band was observed earlier in the PL spectra of InAs nanocrysals grown on Si wafers by MBE [1] or synthesized by high-fluence ion implantation of In and As into Si [4, 5]. That band was ascribed to InAs nanocrystals. In the experiments under consideration here, the similar band is registered in PL spectra of Si implanted with Sb and Ga ions. Thus, the question about the nature of that band arises. Let us assume that a basic contribution to the luminescence in this energy region arises from charge carrier recombination in GaSb nanocrystals. Then, the luminescence intensity should be higher in the sample with the more perfect crystalline structure which is the one being annealed to the longer time. However, this is obviously not the case. Therefore it is more probable to assume that the discussed band is related to radiative recombination at the nanocrystal/Si interfaces. In such interpretation it may be expected that the frequency of the nanocrystal-related band in the PL spectrum is practically independent of the composition of the nanocrystals and of the method of synthesis (MBE or implantation) and is defined by the nanocrystal/Si interface properties, and quantum confinement in PL is a secondary effect only. It should be noted that in some papers [7–9], the surface states at the nanocrystal Si/SiO_2 interface region were considered to have a great influence on the PL properties and the shift of the PL peak was associated with the change of the interface region. A phononless line of 0.79 eV is observed in both spectra. In our opinion, it is related to the recombination of bound excitons on ion-induced defects [interstitial carbon – interstitial oxygen (C_i–O_i pairs) [10]].

A part of samples was additionally annealed (1100 °C, 1 h) to achieve a better recovery of structure. Figure 4b–f depicts TEM-images of these samples. In this case the crystal precipitates are also observed. It is proved by the presence of Moiré contrast (Fig. 4f). The size of the most of precipitates is in the range of 20–90 nm. Though, there are precipitates with the size up to 120 nm (Fig. 4d). One can see dislocation lines connecting the largest precipitates (marked by arrows at Fig. 4c and e). It should be noted ''lighting'' of nanocrystal/Si interfaces at dark-field image (Fig. 4e). The same effect was observed for the samples annealed at 900 °C for 45 min (Fig. 3c). A clearance of observed effect's nature is a subject of further investigations. After the annealing at 1100 °C the band at 0.75–1.05 eV disappears from the PL spectrum (Fig. 2b). As for the samples annealed at 700 °C, the intensive band of exciton emission in Si at 1.09 eV and less intensive bands at 1.03 and 1.14 eV are registered in a PL spectrum of the samples processed at 1100 °C.

In order to identify nanocrystals RS was used. Figure 5 depicts RS spectra of as-implanted and annealed samples.

The Raman spectrum of an as-implanted sample (curve 1) reveals a narrow peak at 512 cm^{-1} corresponding to zone-center phonons scattering of crystalline silicon. The presence of this peak confirms the crystalline state of the silicon matrix after the high-fluence implantation of heavy Sb and Ga ions at elevated temperature. It should be noted that a significant shift toward low frequencies occurs in comparison with the peak's position at 521 cm^{-1} for undamaged Si [11]. We suggest that this shift indicates an existence of significant mechanical strains within the implanted layer. Perhaps, that stress is caused by the accumulation of impurity atoms (for the most part, Sb) in the sub-surface layer. Annealing leads to a shift to high frequencies (up to 518 cm^{-1} after processing at 1100 °C) and to an increase of the intensity of the discussed peak. Though, the annealing regimes used in our experiment do not completely eliminate the stress in the implanted layer. We have detected the RS spectrum of the sample annealed at 900 °C for 45 min after the etching of a 190 nm-layer from its

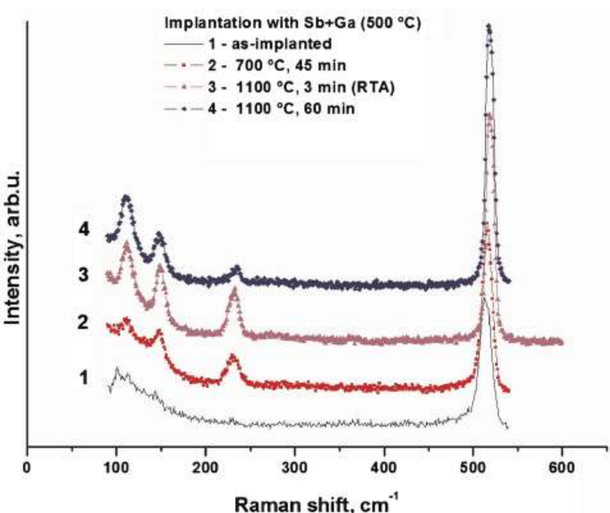

Figure 5 (online color at: www.pss-a.com) RS spectra of Si samples implanted with Sb and Ga and annealed in different modes.

© 2011 WILEY-VCH Verlag GmbH & Co. KGaA, Weinheim

surface and registered the position of discussed peak at 521 cm^{-1} as for un-damaged Si (not shown). Hence, the thickness of the stressed layer is lower than 190 nm.

This stress can be taken into account by assuming a model in which the residual stress is uniformly distributed in the scattering volume [12–14]. In such a case, the stress does not affect the shape of the Raman spectra [15], and the only effect of stress is a shift of the spectra. According to this treatment, the wave number of the first order Raman band in the stressed layer, w_p is shifted in relation to the wave number of the first order Raman band in the absence of stress effects, w_0. This latter parameter corresponds to the position of the Raman line from stress free crystalline silicon (521 cm^{-1}). Then the stress induced shift is given by [12]:

$$\Delta w_s = w_0 - w_p. \quad (1)$$

On the basis of an in-plane stress model, we can estimate the magnitude of such stress, σ to be proportional to the stress induced wave number shift Δw_s [15, 16]:

$$\sigma(\mathrm{MPa}) = 250\Delta w_s(\mathrm{cm}^{-1}). \quad (2)$$

According to this formula, the tensile stress amounts to 2.25 GPa for as-implanted samples and to 750 MPa for samples annealed at 1100 °C. A compressive stress should induce a shift to high frequency.

The annealing results in the appearance of additional bands in the frequency region of 110–235 cm^{-1} in RS spectra. The peak at 233 cm^{-1} is attributed to LO-phonon scattering of crystalline GaSb [11]. Its intensity changes with annealing temperature and duration and its largest value occurs for the sample processed at 1100 °C for 3 min. Additional peaks at 112 and 149 cm^{-1} are registered in RS spectra of annealed samples which are the characteristic lines for Sb. We attribute them to LO- and TO-phonon scattering of crystalline Sb. For bulk Sb the frequencies of LO- and TO-phonons are 113 and 152 cm^{-1} [17], respectively. Probably, the thermal processing of the samples with high Sb and Ga concentrations leads to the formation of both GaSb and Sb precipitates within the Si matrix. A similar situation was reported by other authors for Si implanted at 500 °C with high fluence of As and In ions [4]. After annealing both InAs and crystalline In precipitates were detected by X-ray diffraction.

4 Conclusions We have demonstrated a possibility to produce GaSb nanocrystals in Si by means of high-fluence implantation of Sb and Ga ions and thermal processing. Implantation at 500 °C with Sb (250 keV, 5×10^{16} cm^{-2}) and Ga ions (350 keV, 5×10^{16} cm^{-2}) followed by annealing (900 °C, 45 min) resulted in the formation of GaSb-phase precipitates with sizes from 5 to 60 nm. Thermal treatment at 1100 °C leads to the growth of precipitate sizes to 20–90 nm. The tensile stresses in implanted layers were calculated from RS data. These stresses are attributed to accumulation of Sb atoms in the sub-surface layer and amounts to 2.25 GPa in as-implanted samples and to 750 MPa for samples annealed at 1100 °C. It was found that the low-temperature PL spectrum of Si with nanocrystals depends on thermal processing. For samples after annealing at 900 °C a broad band in the region of 0.75–1.05 eV is registered. For samples processed at 700 or 1100 °C the narrow band of exciton emission in Si at 1.09 eV and bands at 1.03 and 1.14 eV are observed.

Acknowledgements This work was partly supported by the Belarusian Republican Foundation for Fundamental Research (grants F10R-143 and T10R-142).

References

[1] R. Heitz, N. N. Ledentsov, D. Bimberg, A. Yu. Egorov, M. V. Maximov, V. M. Ustinov, A. E. Zhukov, Zh. I. Alferov, G. E. Cirlin, I. P. Soshnikov, N. D. Zakharov, P. Werner, and U. Gösele, Physica E **7**, 317 (2000).

[2] M. Jo, N. Yasuhara, Y. Sugawara, K. Kawamoto, and S. Fukatsu, Abstracts of European Mater. Res. Soc. Spring Meeting: Materials Science and Device Issues for Future Si-based technologies, Strasbourg (France), May 31–June 3, 2005 D/PI. 37.

[3] F. F. Komarov, L. A. Vlasukova, O. V. Milchanin, P. I. Gaiduk, V. N. Yuvchenko, and S. S. Grechnyi, Vacuum **78**, 361 (2005).

[4] A. L. Tchebotareva, J. L. Brebner, S. Roorda, and C. W. White, Nucl. Instrum. Methods Phys. Res. B **175–177**, 187 (2001).

[5] F. Komarov, L. Vlasukova, W. Wesch, A. Kamarou, O. Milchanin, S. Grechnyi, A. Mudryi, and A. Ivaniukovich, Nucl. Instrum. Methods Phys. Res. B **266**, 3557 (2008).

[6] A. Meldrum, S. Honda, C. W. White, R. A. Zuhr, and L. A. Boatner, J. Mater. Res. **16**, 2670 (2001).

[7] Y. Kanemitsu and S. O. Kamoto, Phys. Rev. B **56**, R1696 (1997).

[8] Y. N. Dinh, Y. Y. Chase, M. Balooch, W. J. Siekhaus, and F. Wooden, Phys. Rev. B **54**, 5029 (1996).

[9] X. D. Zhou, F. Ren, X. H. Xiao, G. X. Cai, and C. Z. Jiang, Nucl. Instrum. Methods Phys. Res. B **267**, 3437 (2009).

[10] R. Souer, J. Weber, J. Sholz, E. K. Weber, K. H. Kusters, and H. Alexander, Appl. Phys. A **36**, 1 (1985).

[11] M. Landölt and J. Börnstein, Numerical Data and Functional Relationships in Science and Technology, New Series (Springer-Verlag, Berlin-Heidelberg, 1982).

[12] H. Xia, Y. Z. He, Z. C. Wang, W. Zhang, X. N. Ziu, X. K. Zhang, and D. Feng, Appl. Phys. **78**, 6705 (1995).

[13] M. Yang, D. Huang, P. Hao, F. Zhang, X. Hou, and X. Wang, Appl. Phys. **75**, 651 (1994).

[14] J. Macia, E. Martin, A. Perez-Rodrigues, J. Jimenez, J. R. Morante, B. Aspar, and J. Margail, Appl. Phys. **82**, 3730 (1997).

[15] E. Anastassakis and E. Yiarokapis, Appl. Phys. **62**, 3346 (1987).

[16] E. Anastassakis, in: Physical Problems in Microelectronics, Proceedings of the 4th International School ISPPM, edited by J. Kassavod (Varna, Bulgaria, 1985), p. 128.

[17] Analytical Applications of Raman Spectroscopy, edited by M. J. Pelletier (Blackwell Science, Cambridge, MA, 1999), p. 478.

© 2011 WILEY-VCH Verlag GmbH & Co. KGaA, Weinheim